Molecular Crystals and Liquid Crystals Science and Technology. Section A. Molecular Crystals and Liquid Crystals

Publication details, including instructions for authors and subscription information:
http://www.tandfonline.com/loi/gmcl19

Nematic-Smectic B Interface. Equilibrium and Growth Properties

Tibor Táth Katona [a] & Ágnes Buka [a]

[a] KFKI, Research Institute for Solid State Physics of the Hungarian Academy of Sciences, H-1525, Budapest, P.O.B. 49, Hungary

Version of record first published: 23 Sep 2006.

To cite this article: Tibor Táth Katona & Ágnes Buka (1995): Nematic-Smectic B Interface. Equilibrium and Growth Properties, Molecular Crystals and Liquid Crystals Science and Technology. Section A. Molecular Crystals and Liquid Crystals, 261:1, 349-369

To link to this article: http://dx.doi.org/10.1080/10587259508033481

Mol. Cryst. Liq. Cryst. 1995, Vol. 261, pp. 349–369
Reprints available directly from the publisher
Photocopying permitted by license only

NEMATIC-SMECTIC B INTERFACE. EQUILIBRIUM AND GROWTH PROPERTIES

Tibor Tóth Katona and Ágnes Buka

KFKI, Research Institute for Solid State Physics
of the Hungarian Academy of Sciences
H-1525 Budapest, P.O.B.49, Hungary

ABSTRACT

The equilibrium morphology of the nematic (N) - smectic B (SmB) interface, and its growth properties have been studied in quasi-twodimensional geometry. After thermal equilibration at the $N - SmB$ phase transition temperature T_{NS} two different equilibrium shapes of the SmB phase were found, depending on its orientation. The surface tension anisotropy has been determined from the shape anisotropy of the smectic body. An interesting "inverse process" has been detected in melting of the rapidly grown smectic phase. The stable nematic phase nucleated substancially below T_{NS}. Most of these nematic germs had uniform oval shape, totally different from that of the equilibrium smectic seed. The morphology of the growing smectic B phase in a supercooled nematic also has been studied. Different morphologies were observed, depending on the substance, undercooling $\Delta T = T_{NS} - T$, and alignment of the growing SmB germ. In order to compare the growth dynamics, the area of the patterns was measured and the square root of it versus time was plotted.

1 Introduction

In the natural world a large number of macroscopic shapes appear when a nonequilibrium system grows. Let us mention only a few examples: growth of snowflakes, solidification of metals, formation of coral reefs, dielectric breakdown, electrodeposition, etc. Recent developments in theoretical and experimental research offer the hope that this very different pattern formations can be described by a unified theory.

Pattern growth may be determined by taking into consideration the microscopic interfacial dynamics and the macroscopic external forces simultaneously. The final shape of the pattern results from the competition between them. Most of the investigations are related to *diffusion limited growth*, where the macroscopic dynamics is determined by a diffusion field. In this systems the shapes of the patterns may be grouped into a small number of "essential" shapes as faceted, dendritic, dense-branching [1]. One of the fundamental questions is how the microscopic dynamics influences the macroscopic shape? A complete, corresponding answer does not exist yet, but many significant steps were done in this direction.

Ivantsov [2] showed for a solid forming from its undercooled melt, that the solution of thermal-diffusion and energy-conservation equations gives a continuous family of parabolic crystal fronts with $\rho v = const$ for given undercooling in absence of surface tension and surface dynamics (ρ is the dendrite's tip radius and v is its growth velocity). In contrast, experimentally was proved, that ρ and v are uniquely determined by the undercooling. Moreover, dendrite tips in Ivantsov solutions are

unable to maintain their shape during growth, on the contrary of the experimentally observed stable dendritic growth.

Introduction of surface tension as a perturbation to the Ivantsov solution led to the prediction of a maximum in the $v(\rho)$ curve and to the *maximum-velocity hypothesis* [3]. This hypothesis was also disproved by experiment [4].

More sophisticated investigations were done in the last decade with a more complete incorporation of microscopic dynamics. These studies showed that surface tension and surface kinetics destroy the continuum of Ivantsov solutions, replacing it with a discrete set. All of these allowed solutions, except the fastest one, are linearly unstable, and the growth velocity of this single solution critically depends on the anisotropy of the surface tension ε [5, 6, 7, 8]. This *microscopic-solvability theory* (MST) means that the surface tension, its anisotropy, and the surface kinetics, if they are incorporated from the beginning, may totally change the character of the solutions.

For example, when the surface tension and the surface kinetics are isotropic, instead of dendritic growth the tip splitting fingers arise, leading to the *dense branching morphology* (DBM). By the experiments, as solidification from undercooled melt [9], growth in Hele-Shaw cell (viscous fingering) [10, 11, 12], supersaturation [13, 14], growth by electrochemical deposition [15, 16], it was verified that, in the absence of significant anisotropy, the tip-splitting is the selected growth mode. This tip-splitting results from the competition between macroscopic diffusion field and the microscopic effects of isotropic surface tension and surface kinetics. The macroscopic diffusion field tends to make the interface irregular. On the other hand, isotropic surface tension and surface dynamics have a stabilizing effect, tend to keep a velocity uniform and the interface smooth. In the absence of this stabilizing effect at the interface (without surface tension and surface kinetics), the diffusive Mullins-Sekerka [17] instability causes an unstable interface - the *fractal growth* appear. It was seen in the modelling of growth without surface tension [18, 19, 20, 21] and in fluid flow experiments with two miscible fluids [22], where the surface tension was very small.

After the experimental proof with anisotropic Hele-Shaw cell [10], the role of anisotropy in formation of stable parabolic dendrites is widely accepted. The first recognition, that anisotropy is required to produce dendritic growth, dates from two simple models of interfacial growth [23, 24]. One of these, the *boundary layer model* (BLM) was built on solidification from an undercooled melt [23]. This BLM simplifies the diffusion problem by assuming that the entire temperature change occurs within a narrow layer near the interface [1]. The role of anisotropy can be demonstrated on the following way. On the crystal solidifying with a parabolic interface and a finite surface tension, the coldest point is the tip according to Gibbs-Thompson relation:

$$T_i = T_m - (\frac{L}{c_p})d_0\kappa - \beta v^\alpha, \tag{1}$$

where: T_i - temperature of curved parts of the interface,

T_m - melting temperature of a flat interface,

L - latent heat of the liquid-solid transition,

c_p - heat capacity of the liquid at constant pressure,

$d_0 = \sigma T_m c_p / L^2$ - the capillary length,
σ - the surface tension,
κ - the local curvature of the interface,
βv^α - the kinetic term.

Relation (1) describes a heat gradient between the side and the tip of the parabolic interface, which have different local curvatures, consequently the heat flows towards the tip, slowing down the advance of the interface. In the same time, cooling of points at the sides of the tip causes these points to overtake the tip and the tip splitting growth arises.

In the presence of anisotropy the surface tension σ in relation (1) will be replaced by the surface stiffness $\sigma(\theta) + \sigma''_{\theta\theta}$. The tip is no longer the coldest point along the interface and a competition developes between the anisotropy and the shape selection of the needle crystal. The *microscopic solvability criterion*, that only the fastest growing needle crystal can survive the effect of the diffusive instability, was discovered using the geometrical model [25] and the boundary layer model [26]. Meiron [27], also showed from numerical integral formulation, that anisotropy is necessary for stable growth of the tip of a needle crystal with constant velocity.

However, the experiments with anisotropic Hele-Shaw cell [10], Hele-Shaw cell using liquid crystal as the viscous fluid [11, 12], electrochemical deposition [15, 16], solidification from supersaturated solutions [10] and solidification of water [9] exposed a new problem. In these experiments dendrites are not always observed when anisotropy is present. As the driving force is decreased the tip splitting arises below a critical value. As a solution of this problem Ben-Jacob et al. [28] proposed the *fastest growing selection hypothesis*, that it is the fastest growing morphology which is the dynamically selected one.

Despite all its advantage, the microscopic solvability theory also has some deficiencies. The set of equations is difficult to solve and it is possible only with approximations. The theory is most well-developed for two dimensions, but experimental dendrites are usually three dimensional. Upon that, this theory ignores the effects of microscopic crystal structure and growth kinetics, moreover does not include the effects of sidebranching.

The surface tension anisotropy (precisely, the normalized angle dependent function $\sigma(\theta)$) can be obtained from the equilibrium shape of the solid-liquid interface by the Wulff construction [29]. By our knowledge, experimentally determined surface tension anisotropy has been reported only for few materials with rather poor reproducibility. Repeated measurements of pivalic acid's surface tension anisotropy, for example, showed different values within an order of magnitude (see [30]). In liquid crystals, P.Oswald et al. [31] measured the surface free energy of a Smectic B germ in contact with a Smectic A phase for butiloxybenzilidene octylaniline, by using the Wulff construction and the. Naito et al. [32] performed the calculations for Smectic A-Isotropic interface in equilibrium. Investigations of the equilibrated SmB-N interface was done by Buka et al [33].

With the sufficient computer technology for the numerical integration of the unsteady equations, in the past few years a new approach appeared to the problem of the pattern formation. Langer [34] invented the *phase field model of solidification*, based on an entropy functional formulation. For the solidification of a pure material,

the model departs from the Landau-Ginzburg free-energy functional:

$$\mathcal{F} = \int_{\Omega} [f(\Phi, T) + \frac{1}{2}\varepsilon^2(\nabla\Phi)^2]d\Omega, \tag{2}$$

where Ω is the region occupied by the system, $\Phi(\mathbf{x}, t)$ is the phase field, $T(\mathbf{x}, t)$ is the temperature, $f(\Phi, T)$ is the free energy density and ε is a parameter which includes the anisotropy of the system (and which is constant for an isotropic material).

As result the phase-field method produces many of the qualitative features observed in real crystal growth. Numerical solutions of Wheeler et al. [35] show dendrite formation for growth into an undercooled melt and demonstrate the importance of the magnitude of surface tension anisotropy. Quantitatively they found a reasonable agreement to the Ivantsov solution and to MST for a fixed value of the interface thickness, however the results depend on the interface thickness. Probably the largest advantage of the phase field model is that the location of the solid-liquid interface does not have to be determined explicitly, and with further development of the numerical solution techniques we can expect better results in growth simulation.

Finally, let us emphasize some advantages of using the liquid crystals compared to the other materials in order to investigate pattern formation during solidification. First of all, the transport is faster than in crystals, so the equilibration time is much shorter. Besides, liquid crystals exhibit large anisotropies, they are transparent and birefringent, moreover melt at low temperature. These features make them extremly convenient for experimental studies of different pattern forming processes.

2 Experimental

Four liquid crystalline substances were used for observations. Each of them have a first-order phase transition nematic to smectic B at T_{NS}:

I. 4-n-propyl-4'-cyano-trans 1,1-bicyclohexane, $T_{NS} = (56.3°C)$

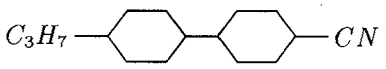

II. 4-n-pentyl-4'-cyano-trans 1,1-bicyclohexane, $T_{NS} = (51.2°C)$

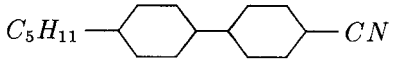

III. 4-n-butyl-N-[4-(p-cyanophenyl)-benzilidene]-aniline, $T_{NS} = (87.4°C)$

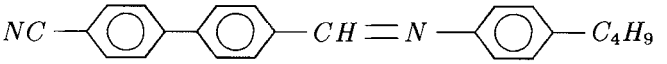

IV. 4-n-propyl-4'-trifluoromethoxyphenyl-ethylene-trans 1,1-bicyclohexane, $T_{NS} = 77.0°C$

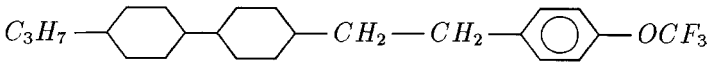

Substances I, II, and III show monotropic SmB transition, while IV exhibits the phase on cooling and on heating from below.

The $N - SmB$ phase transition (smectification), we studied, is the liquid crystalline analogy of solidification of a pure substance. The diffusion field was thermal in our observations. The sample temperature was controlled in a hot stage with accuracy of $0.002^{o}C$. The hot stage was mounted on a polarizing microscope equipped with CCD video camera. The recorded images were fed into a PC for digital analysis, with spatial resolution of 512x512 and 256 gray scaling for each pixel. For the calibration of the system i.e. for the determination of the pixel dimensions, the squared net of a Bürker-chamber has been used. With 6.3× objective and 1.6× projector combination the scale factors of $1.35\pm0.01\mu$m/pixel in x direction and $0.95\pm0.01\mu$m/pixel in y direction were determined, so the calculated area of the pixel is $1.28\pm0.02\mu m^2$.

Samples of both surface alignments of the nematic phase - planar (P) and homeotropic (H) - were prepared in cells of dimensions $10x10mm^2$ and of thickness d=10μm. The only exception was substance IV, for which homeotropic orientation could not be achieved. For planar orientation of the nematic phase we used commercial liquid crystal cells manufactured by E.H.C. Co., Ltd. (Japan). For making cells with homeotropic orientation the glass plates with SnO_2 coating have been used. A thin layer of octadecyl-triethoxy-silane, transferred onto the inner surfaces by polymerization, assured the homeotropic alignment.

	ORIENTATION					
	P(inP)	P(inH)	H(inH)	H(inP)	T(inP)	T(inH)
Substance I	●	●	●			
Substance II	●	●	●	●	●	●
Substance III	●	●	●			
Substance IV	●					

TABLE 1. *Different orientations of the SmB phase in nematic surrounding. The first letter is related to the SmB phase while the letter in parenthesis shows the nematic alignment.*

During experiments different director orientations of the SmB phase were found: planar (P), homeotropic (H) for all investigated substances, and in addition tilted (T) for substance II. In order to easier treatment of the both (SmB and N) phase orientations we introduced *symbols*. Thus, for example in case of planarly oriented smectic germ in homeotropic nematic surrounding, we used designation P(in H), etc. (see also [36]). Table 1 shows the different director configurations on both sides of the $N - SmB$ interface.

3 Results

3.1 Nematic-Smectic B Interface in Equilibrium

In order to determine the equilibrium shape of the $N - SmB$ interface, the SmB phase has been heated up by slowly approaching T_{NS}. Before the last SmB germ dissapeared, the heating was stopped. After that this germ was grown very slowly by decreasing the temperature and then kept at *fixed* size (at the phase transition temperature T_{NS}) with small temperature corrections. After thermal equilibration at T_{NS} of about 1 day, two totally different equilibrium shapes of the smectic body (in nematic surrounding) were found, depending on the director orientation of the smectic seed (Fig.1). In case of planarly oriented smectic germ in a planar nematic surrounding - P(in P) configuration - the SmB shape was a very elongated rectangle with faceted long sides and convex short ones (Fig 1a). The faceted sides were parallel with the smectic layers and perpendicular to the director. In order to determine the shape anisotropy we measured the quantity: $\varepsilon = (R_{max} - R_{min})/(R_{max} + R_{min})$, which coincides with the surface tension anisotropy $\varepsilon = (\sigma_{max} - \sigma_{min})/(\sigma_{max} + \sigma_{min})$,

where: R - distance of the germ perimeter from its nucleation point,

σ_{max}, σ_{min} - highest and lowest value of the normalised surface tension [14, 30].

In P(in P) alignment we measured very large values of ε: 0.68 for substance I [36], and 0.94 for substance II [37].

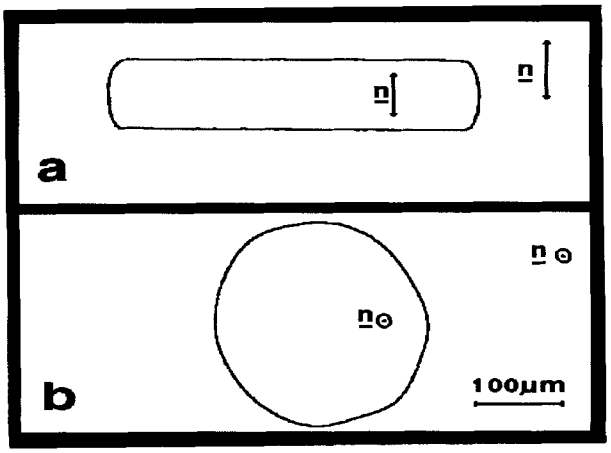

FIGURE 1. *Experimental equilibrium shapes of the SmB germ in nematic surrounding obtained after digital processing of the images for substance I. Double arrows represent the director orientations* **n**. **a**. P(in P), **b**. H(in H) *configuration.*

Similar morphology was found for P(in H) configuration with somewhat smaller anisotropy. The difference is, that the surrounding nematic is homeotropic, thus the director orientation changes by an angle of 90 degrees between two sides of the $SmB - N$ interface. Because of this change in the orientation, an elastic deformation

of the nematic phase occurs near the interface. It has been shown [33], that the additional contribution to the surface energy coming from the elastic deformation should lead to the smaller anisotropy of the equilibrium shape. This assumption was proved experimentally: we measured the value $\varepsilon = 0.49$ for P(in H) in substance I.

A totally different type of shape was found in H(in H) configuration. Here, the director orientations of both N and SmB phases were perpendicular to the plane of the picture (Fig.1b). In this case the shape of the smectic body was circular with a small hexagonal modulation, $\varepsilon = 0.03$ for substance I.

In each investigated substance the above described equilibrium shapes of the SmB germ were found with slightly different values of ε. In addition, there are three more configurations, observed only in substance II. One of these is H(in P) and the others are T(in H) and T(in P), where the director orientation of the SmB phase is tilted [37].

From the shape of the equilibrium smectic body the angle dependence of the surface tension $\sigma(\theta)$ was determined by the Wulff construction and reported in [36].

3.2 Spontaneous Nucleation of the Smectic B Phase

As we mentioned all investigated substances have a first order phase transition nematic to smectic B and the nematic phase of the samples could be supercooled.

For small undercoolings ($\Delta T < 0.2°C$) of the nematic phase no spontaneous nucleation of SmB occured on time scale of hours. At larger ΔT the fast, spontaneous dendritic growth of the planarly oriented smectic B germ has been detected, with four main branches (Fig.2a) for substances I and IV. The angle between these branches was about 90°. In case of substance II the growing planar SmB germ had a shape of very elongated rod (Fig.2b) - without the above mentioned four main branches. The growth velocity v of the dendrite tip was found constant in time and it varied in the range of $v = 80-300\mu m/s$, depending on substance and undercooling [36].

Substance III exhibited a very high nucleation activity with respect to the other substances. Morphologically (Fig.2c) had a similar behaviour as substances I and IV, but the growth velocity of the tip was not constant, it decreased with time as $v \sim t^{-\alpha}$ where α is about 0.9 [38]. Besides, the found initial value of v for substance III was much smaller ($v \sim 2 - 10\mu m/s$), so the growth process was very slow compared to the other substances. If we compare Figures 2a and 2c, it can be also seen, that substance III has less developed side branches than substance I (and IV).

This observations were carried out with both surface aligned - planar and homeotropic - nematic phases. It is surprising that spontaneously nucleated SmB germs always grow with planar orientation, independently from the orientation of the nematic surrounding (planar or homeotropic). Moreover, we tried to influence the orientation of the nucleating smectic body by applying an electric field perpendicular to the glass plates with homeotropic surface treatment. Since all investigated substances have strong positive dielectric anisotropy, we expected the homeotropic

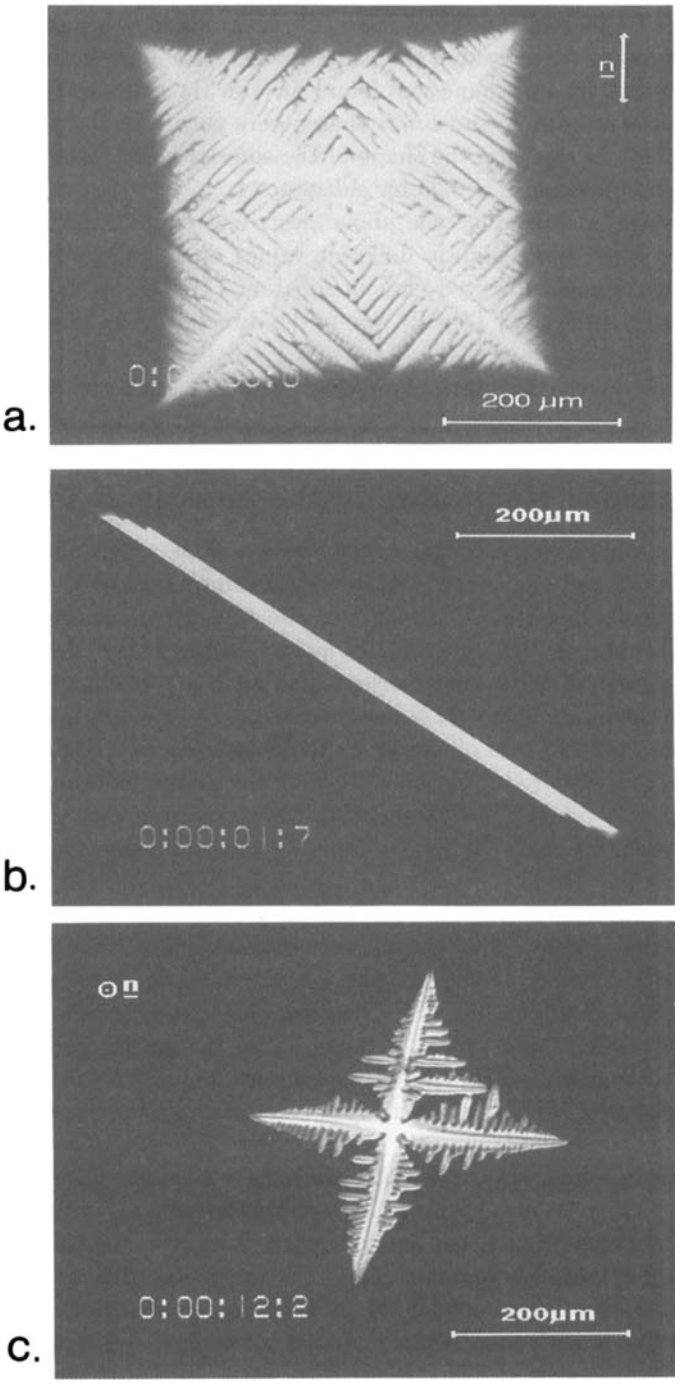

FIGURE 2. *Spontaneous nucleation of the SmB germ.* **a.** *Substance I,* **b.** *Substance II,* **c.** *Substance III.*

alignment for the nucleating smectic seed. Nevertheless the germs turned over to be planar up to a field $50V/10\mu$m. It is very strange, because we obtained the homeotropic orientation of the SmB germ relatively easily, by thermal manipulation of a *preserved seed* (see below). In any case, the morphology and the growth regime of the spontaneously nucleated smectic germ seems to be independent from the orientation of the nematic surrounding.

3.3 Growth of Preserved Smectic B Germ

As we mentioned above in case of spontaneous nucleation of SmB phase, only the fast dendritic growth with planar - P(in P) or P(in H) - orientation was observed. For precise quantitative measurements we used the same germ which was kept "alive" during several cooling and heating cycles. In this way we could perform measurements with lower undercoolings and on the other hand investigate the H(in H) configuration. Namely, in cells with homeotropic surface treatment, by melting the planar smectic phase (which was obtained by spontaneous nucleation) till the last remained germ gets smaller than the sample thickness, the germ turns over to homeotropic orientation influenced by the homeotropic nematic surrounding. Then applying a fast cooling before the germ disappeares, due to the large undercooling the homeotropic germ grows rapidly without having the chance to turn back again and in such way the H(in H) configuration can be obtained. If the dimensions of the initial planar germ is not smaller than the thickness of the cell the seed remains planarly oriented.

In this way, with appropriate thermal manipulation of a preserved smectic seed the growth properties of it could be studied in detail for P(in P), P(in H) and H(in H) $N-SmB$ configuration. Three others H(in P), T(in P) and T(in H) orientations, found only for substance II [37], will not be discussed here.

In general, three growth regimes have been found as a function of undercooling ΔT for all configurations and for all investigated substances. This regimes could be clearly distinguished in the morphology and in the time dependence of the growth velocities $v(t)$ also. The only exception was substance III, which had a similar morphological behaviour as the other materials, but its $v(t)$ had a form $v \sim t^{-\alpha}$ for all regimes and for any configuration (with various α) [38].

Because of the very different morfologies of the $N-SmB$ interface we found, the area A of the pattern has been measured and we plotted the square root of it versus time. In this way we can compare the growth dynamics of patterns for any shapes. Results of these investigations for different growth regimes will be presented in the following subsections for all three configurations - P(in P), P(in H) and H(in H). Most of data analyses and morphological descriptions will be given for substance I. The occasional differences for the other substances will be given.

I. *SLOW GROWTH REGIME*

In a small range of undercooling just below T_{NS} ($\Delta T < 0.1^{\circ}C$) a slow growth of SmB germ called *quasi-equilibrium regime* has been observed. The shapes of the

growing smectic patterns are not much different from those in equilibrium state. In P(in P) and P(in H) configurations the long sides of the germs stay faceted, till the short ones become less convex (Fig.3a). The shape anisotropy ε increases with time, which is shown on the Figure 4. The H(in H) pattern at the beginning has a circular shape with small hexagonal modulation. After reaching an area of the order of $10^5 \mu m^2$ the form of the germ will be irregular - "puddle-shaped" (Fig.3b).

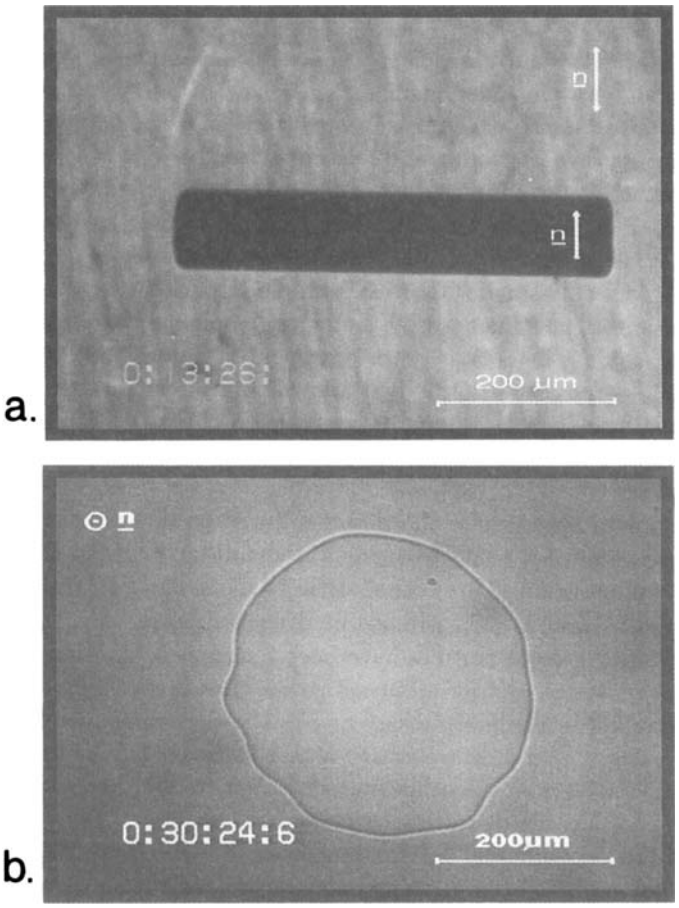

FIGURE 3. *Typical shapes of the SmB germ in slow growth regime.* **a.** *P(in P) geometry and* **b.** *H(in H) configuration (both for substance I).*

Figure 5 shows the measured values of the square root of germ area versus time for all three configurations. From the graph it is visible that the growth velocity decreases with time in this regime for all $N - SmB$ alignments. The maximum of the growth velocity, which coincides with the initial value (if we neglect the transient effect) has an order of magnitude $v \sim 1 - 2\mu m/s$.

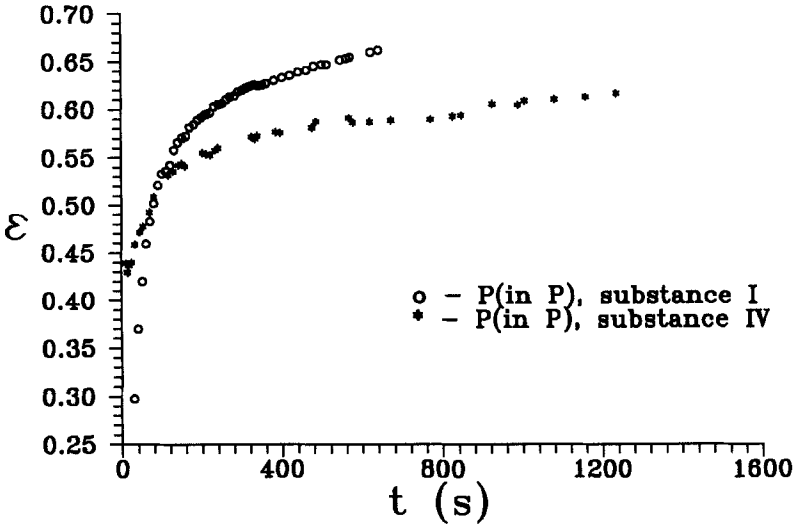

FIGURE 4. *Time dependence of the shape anisotropy ε in the slow growth regime ($\Delta T < 0.1°C$) for the planar SmB germ.*

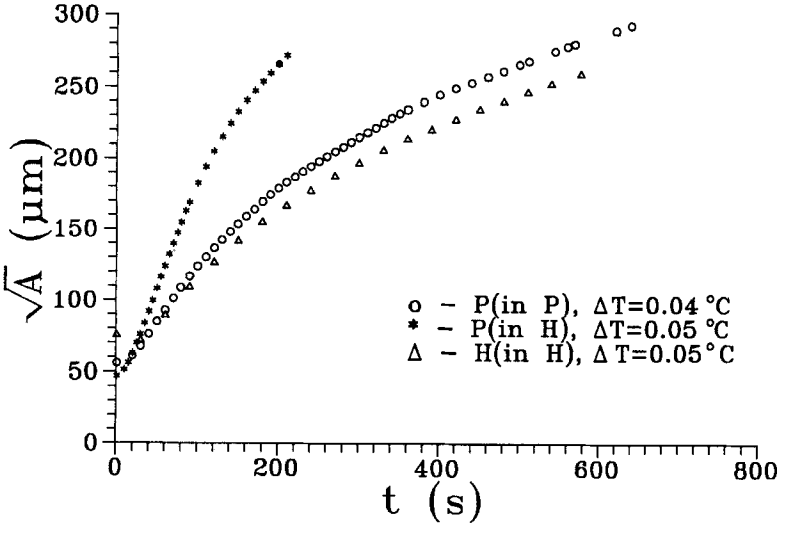

FIGURE 5. *Time dependence of the square root of the germ area in slow growth regime for substance I.*

II. *INTERMEDIATE GROWTH REGIME*

In the range of undercooling: $0.1°C \leq \Delta T < 0.2°C$ another growth regime arises.

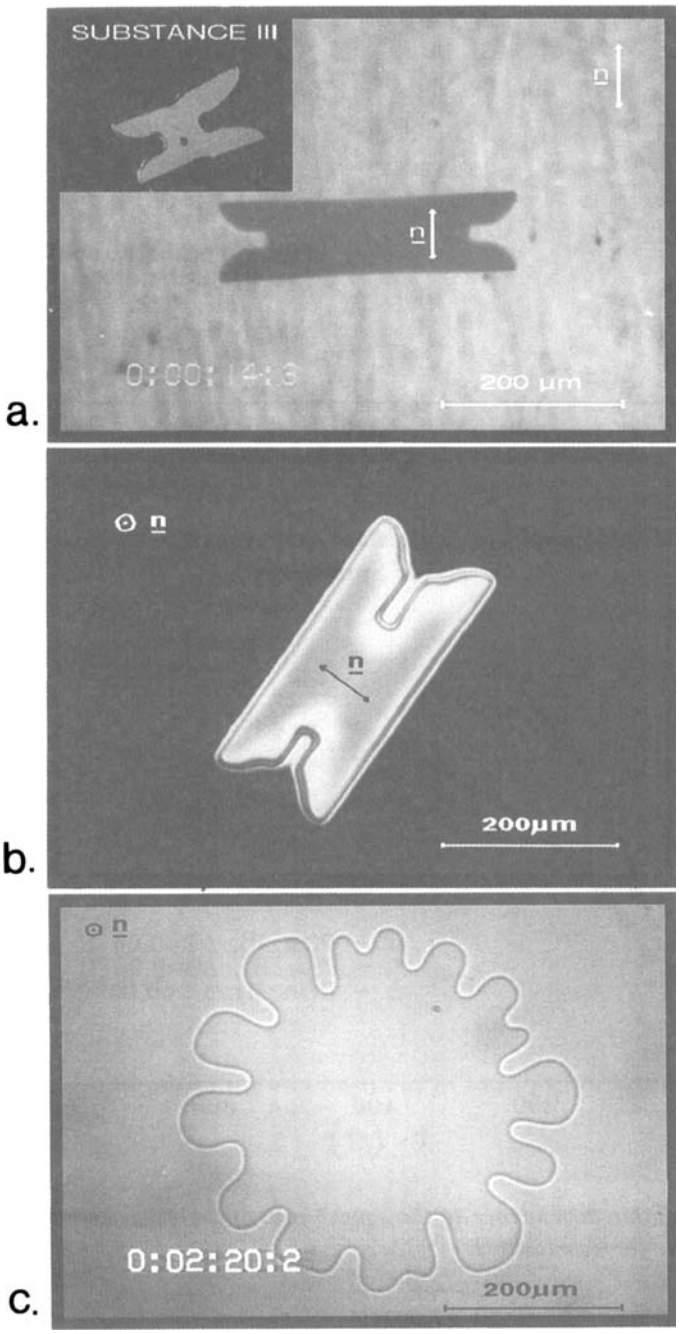

FIGURE 6. *Shapes of the SmB germs in the intermediate regime.*
a. *P(in P) configuration for substance I. The upper left corner with black background shows the SmB germ in case of substance III.*
b. *P(in H) geometry for substance I.*
c. *H(in H) configuration of substance I*

For the P(in P) and P(in H) germs the short sides become *concave*, while the long sides remain faceted. In this regime the forming of four main branches occured, which grew parallel with the smectic layers (Fig.6a and b). The upper left corner of Figure 6a (the black field) shows the shape of the planar SmB germ of substance III. For this substance the destabilization of the faceted sides also has been observed in this regime. From the Figure 6b it is possible to see the deformation zone at the $N - SmB$ interface in the nematic phase. In this zone the director turns over from homeotropic (in N) to planar (in SmB) orientation. The morphology of the H(in H) germ is also changed in this growth regime - fingers appear and the nonequilibrium growth begins (Fig.6c).

Concerning the growth dynamics, as it is shown in Figure 7, the growth velocities of the pattern's area are constant after a transient effect caused by thermal relaxation of the cell. In the figure the values of these constant velocities are given for all configurations.

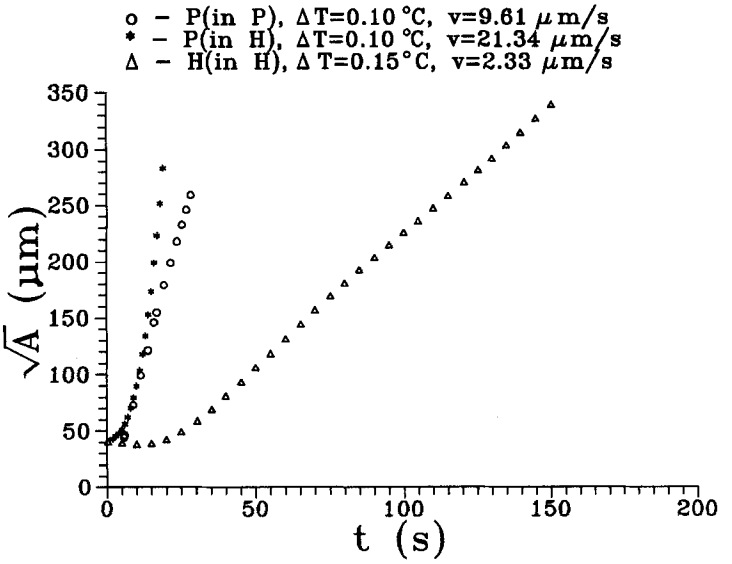

FIGURE 7. *Square root of the area versus time in the intermediate regime for substance I. Growth velocities of the area of the SmB germs given in the picture correspond to the slope of the linear part of the curves.*

As an exception, we want to mention again substance III, the behaviour of which is somewhat different. Though morphologically we could find all growth regimes described in these subsections, the time dependence of the growth velocity always had a form $v \sim t^{-\alpha}$.

III. *FAST GROWTH REGIME*

The fast growth regime has been established not on the base of morphology in the first place, but on the basis of growth dynamics. Namely, for undercoolings

$\Delta T > 0.2°C$, the growth velocity increases with time for all types of germs. It is shown in Figure 9.

The morphology of the P(in P) and P(in H) germs changes continuously with increasing undercooling. For $\Delta T \approx 0.2–0.3°C$ the faceting of the long sides vanishes, the interface becomes rough. The branches open up, but the tip growth remains non-parabolic, because the growth direction of the tip changes with time (Fig.8a). At larger undercooling ($\Delta T \geq 0.5°C$) one gets typical dendritic growth (parabolic tips), with four main branches at an angle of about 90 degrees, not much different from those obtained by spontaneous nucleation (Fig.2a).

For the H(in H) germ a *dense-branching regime* could be observed in the whole range of undercooling $\Delta T > 0.2°C$. The pattern's enveloping curve preserves the hexagonal shape (Fig.8b). Dendritic side branches in the upper right corner of the Figure 8b originate from the spontaneously nucleated (due to the very large undercooling) and planarly oriented *SmB* germs.

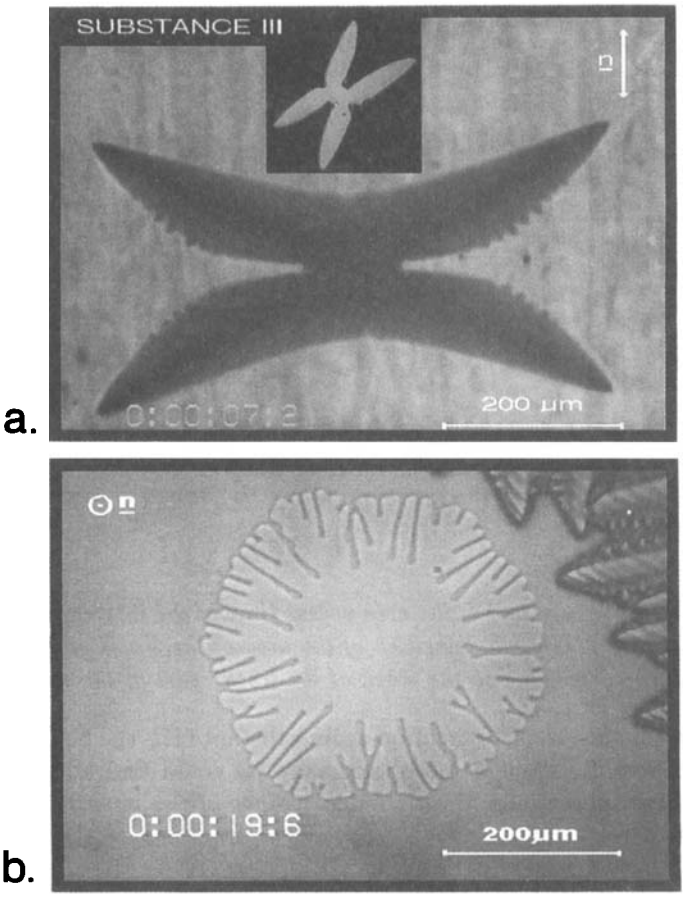

FIGURE 8. *Morphologies of the SmB germ in the fast growth regime.*
a. *Planar smectic seed for substance I,* $\Delta T = 0.3°C$.
b. *H(in H) configuration for substance I,* $\Delta T = 0.9°C$.

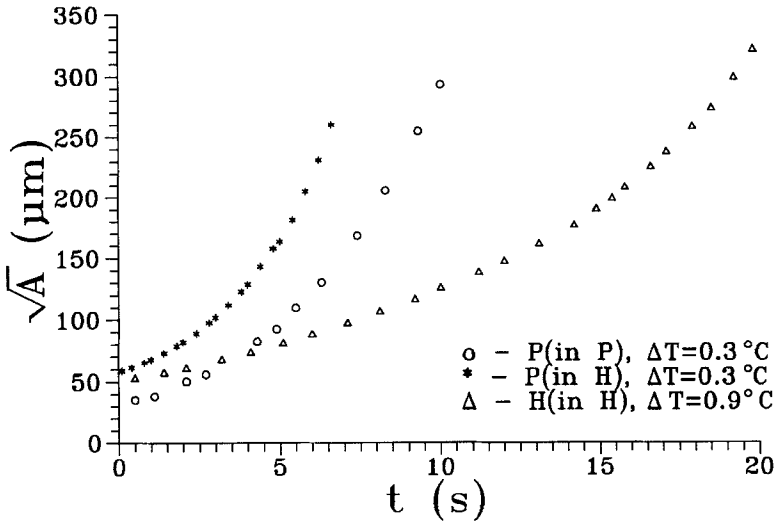

FIGURE 9. *Growth dynamics of the SmB germs in the fast regime for substance I.*

4 Melt of the Smectic Phase - "Inverse Process"

During the investigation of the SmB growth in nematic surrounding a peculiar effect has been observed. At large undercooling the obtained smectic phase contained different SmB domains originated from different germs. When we slowly heated up this smectic phase, the nucleation of the nematic occured below the phase transition temperature T_{NS} (the SmB phase could not be overheated). With stabilization of the temperature at $T < T_{NS}$ the nematic "islands" mostly having an oval shape could be equilibrated with smectic surrounding.

Our first impression was that this coexistence of both phases below T_{NS} is caused by impurities in the samples. However, the influence of the impurities should be reversible, i.e. we should have observed the broadening of the phase transition on cooling of the nematic phase too. On the contrary, the transition was always sharp in cooling from above.

Another possible reason for nucleation of the nematic phase below T_{NS} could be the disorder of the rapidly grown SmB phase. Namely, a small misalignment in director's orientation exists at locations where the side branches collide with each other (see Figure 2a). Such a slightly disordered SmB phase is metastable and it melts below T_{NS}. On the other hand, the misalignment between the smectic domains also exists (the director orientations are different in different domains). This misalignment was smaller in planarly oriented samples (about $\phi \leq 10^{o}$), in comparison to the homeotropic ones. Consequently, the boundaries of the domains would also melt at lower temperature than T_{NS}.

In order to test this, the following experiment has been performed on the planarly oriented sample of the substance IV. In the first step the smectic germ has been grown very slowly (as it is shown in Figure 3a). In this way a faceted and "ordered" (with the homogeneous director orientation everywhere) SmB body of large dimensions has been obtained. After that a large undercooling has been applied in order to get the smectic phase in the whole sample. The "ordered" SmB body was then surrounded with "disordered" smectic domains originated from different spontaneously nucleated smectic germs which had different director orientations. The angles ϕ between director orientations of the "ordered" smectic body and these domains have been measured, and with slow heating we detected the temperatures at which the boundaries with different ϕ became nematic. Results of these studies are presented in Figure 10 for substance IV in P(in P) configuration. The figure shows the phase transition temperature at the domain boundaries as a function of the angle ϕ, for two independent measurements. In spite of large experimental errors, the graph clearly shows the tendency that the melting temperature is lower where the misalignment is larger.

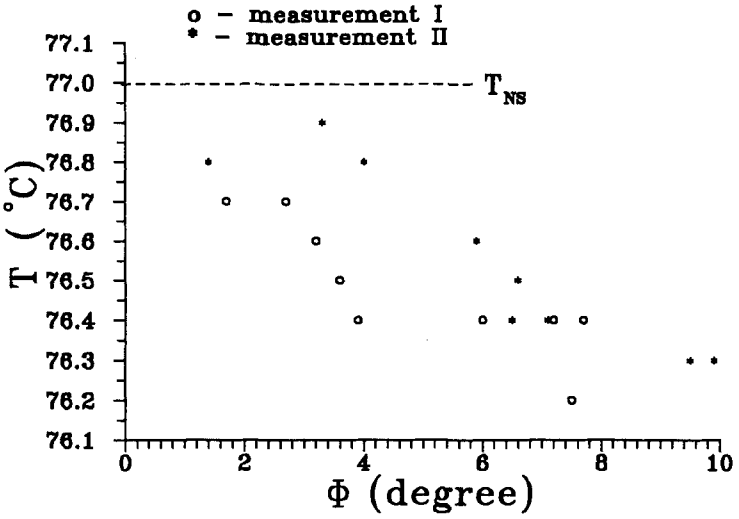

FIGURE 10. *The nucleation temperature of the nematic phase versus angle ϕ, between director orientations of the neighbouring SmB domains for substance IV.*

The most surprising feature of these nematic "islands" is their shapes. Naturally, we expected the same equilibrium shape of the nematic phase in smectic surrounding as it was obtained for the smectic germs in the nematic. However, the equilibration experiments showed the totally dissimilar situation. After thermal equilibration of more than one day, nematic channels between smectic domains, and oval shaped nematic "islands" inside of the domains have been observed, see Figure 11c.

Figure 11a shows planar smectic domains with different director orientations for substance IV ($T_{NS} = 77.0°C$) at $T = 75.0°C$, in P(in P) configuration. With increasing temperature, first a nematic channel has been observed on the domain

boundary, which was parallel to the underlying nematic director at temperature $T = 76.7°C$. At the same temperature the nucleation of the nematic phase is just

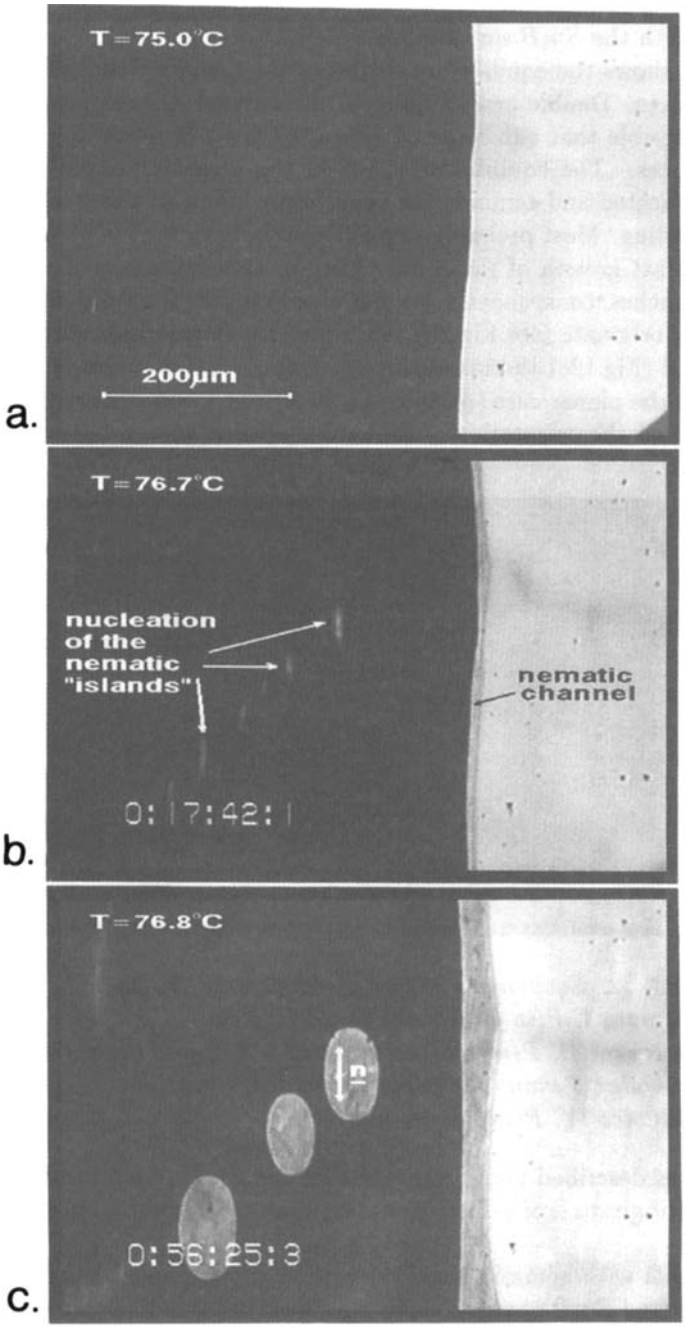

FIGURE 11. *The appearance of the nematic phase on heating the SmB. Double arrow in Fig.c shows the director orientation of the nematic phase.*

starting inside the darker domain where an oblique straight boundary exists between very slightly misaligned regions (Fig.11b). Figure 11c gives the picture at $T = 76.8°C$, where the nematic "islands" were formed and these "islands" stay in equilibrium with the SmB surrounding.

Figure 12 shows the equilibrium shapes of the nematic "islands" for all investigated substances. Double arrows indicate the director orientations of the nematic phase. It is visible that substance II (Fig.12b) behaves quite differently from the other substances. The equilibrium shape of the nematic "island" in case of this substance is faceted and reminds the equilibrium shape of the smectic germ in nematic surrounding. Most probably this different behaviour is in connection with the fact that the fast growth of the SmB phase for this substance is rod-like, without four main branches, consequently without side branches from which the oval shaped germs usually originate (see Fig.2b). We note that in a sample with a homeotropic N background (Fig.12c) the misalignment of the SmB domains is obviously much larger than in the planar case (ϕ can reach 90 degrees), consequently the N channels are irregular and the orientation of the oval shaped islands is uncorrelated.

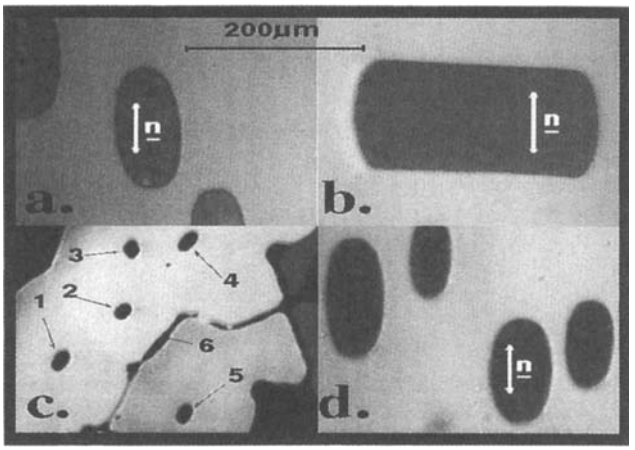

FIGURE 12. *Equilibrium shapes of the nematic "islands".*
a. *substance I, P(in P),* **b.** *substance II, P(in P),*
c. *substance III, P(in H), the numbers 1-5 denote the nematic islands, while number 6 shows the nematic channel,*
d. *substance IV, P(in P).*

All features described above indicate that the SmB phase produced by rapidly growing smectic germs is of a different nature than that produced in quasi-equilibrium growth.

Experiments with nematic phase nucleation showed another important feature. When both N and SmB phases coexist, the SmB phase is thicker near the $N-SmB$ interface than far from it, even if the interface is flat in the plane of the sample. This fact is warning us that the role of the third dimension (the sample thickness) also must be taken into account. Namely, the existence of the local curvature in

this third dimension causes a local decrease of the temperature, according to Gibbs-Thompson relation (1). On account of this temperature decrease, the SmB phase becomes thicker near the flat interface.

We mention that we are lately informed about experimental studies of the substance I, performed by P. Oswald et al. [39]

5 Discussion and Conclusion

In the present paper we give the more complete description of our investigations of the $N - SmB$ interface. Some results of these investigations already have been reported [33, 36].

Concerning the equilibrium shape of the SmB body, we want to mention that it is very difficult to determine the shape anisotropy ε better than about $30 - 40\%$. A possible explanation of this problem is that we obtained the equilibrium shapes by keeping the bodies at *fixed* size with small temperature corrections ($\sim 0.002^oC$) within the range of 0.02^oC, and not at the exact temperature T_{NS}.

For the planarly oriented SmB germ we observed only the dendritic growth in the whole range of undercooling. It shows that this growth is strongly influenced by extremly large anisotropy of the planarly oriented liquid crystal samples.

In case of homeotropic SmB germs only the tip-splitting growth has been observed for substances I and III. For substance IV the homeotropic orientation could not be achieved. Substance II showed the dendritic growth in H(in H) configuration in a small range of undercooling [37]. The absence of the dendritic growth for substances I and III should be explained with small anisotropy of the homeotropic samples, but P. Oswald et al. [40] observed the dendritic growth for a columnar liquid crystal with smaller anisotropy than our substance I. Most probably we did not monitor precisely enough the whole range of undercooling. The more detailed study of this question is in progress.

In general, for all growth regimes, we can see from the Figures 5,7 and 9 that the growth is fastest in P(in H) configuration followed by P(in P) and H(in H) as the slowest one.

On the basis of the investigations of the SmB phase during melt we suggest that the smectic phase is strongly influenced by its thermal history. The rapidly grown phase, by our opinion, has no long-range SmB order and therefore, there is no faceting of the nematic germs. On the other hand, by slow cooling of the initial SmB germ in quasi-equilibrium regime the "ordered" smectic B phase can be obtained.

Finally, let us mention, that first trials of the SmB growth simulation with the phase-field model shows a good agreement with experimental results and are very promising for future studies [41].

6 Acknowledgement

Substance III was synthesized by K.Fodor-Csorba, materials I, II and IV were kindly made available for us by Merck, Darmstadt. The work was financially supported by

the Hungarian Academy of Sciences (OTKA 2976) and the Volkswagen Foundation. Authors wish to thank Prof. L. Kramer for many fruitfull discussions and the Alexander von Humboldt Foundation for the equipment donation.

References

[1] E.Ben-Jacob and P.Garik, Nature, **343**, 523 (1990)

[2] G.P.Ivantsov, Dokl. Akad. Nauk SSSR, **58**, 567 (1947)

[3] J.S.Langer, Rev. Mod. Phys., **52**, 1 (1980)

[4] M.E.Glicksmann, R.J.Shaefer and J.D.Ayers, Metall. Trans., **A7**, 1747 (1976)

[5] D.A.Kessler, J.Koplik and H.Levine, Adv. Phys., **37**, 255 (1988)

[6] E.A.Brener and V.I.Melnikov, Adv. Phys., **40**, 53 (1991)

[7] J.S. Langer, Science, **243**, 1150 (1989)

[8] P.Pelce, Dynamics of Curved Fronts (Academic, New York, 1988).

[9] S.H.Tirmizi and W.N.Gill, J. Cryst. Growth, **96**, 277 (1989)

[10] E.Ben-Jacob, R.Godbey, N.D.Goldenfeld, J. Koplik, H.Levine, T.Müller and L.M.Sander, Phys.Rev.Lett., **55**, 1315 (1985)

[11] A.Buka, P.Palffy-Muhoray and Z.Rácz, Phys.Rev.A, **36**, 3984 (1987)

[12] A.Buka and P.Palffy-Muhoray, Phys.Rev.A, **36**, 1527 (1987)

[13] P.Oswald, J.Phys.(Paris), **49**, 1083 (1988)

[14] A.Dougherty, J. of Crystal Growth, **110**, 501 (1991)

[15] Y.Sawada, A.Dougherty and J.P.Gollub, Phys. Rev. Lett., **56**, 1260 (1986)

[16] D.Grier, E.Ben-Jacob, R.Clarke and L.M.Sander, Phys. Rev. Lett., **56**, 1264 (1986)

[17] W.W.Mullins and R.F.Sekerka, J. Appl. Phys., **34**, 323 (1963); **35**, 444 (1964)

[18] T.A.Witten and L.M.Sander, Phys. Rev. Lett., **47**, 1400 (1981); Phys. Rev.B, **27**, 5686 (1983)

[19] P.Meakin, Phys. Rev.A, **27**, 604 (1983); **27**, 1495 (1983)

[20] J.Nittmann and H.E.Stanley, Nature, **321**, 663 (1986)

[21] L.M.Sander, Nature **322**, 789 (1986)

[22] J.Nittmann, G.Daccord and H.E.Stanley, Nature, **314**, 141 (1985)

[23] E.Ben-Jacob, N.D.Goldenfeld, J.S.Langer and G.Schön, Phys. Rev. Lett., **51**, 1930 (1981); Phys. Rev.A, **29**, 330 (1984)

[24] R.C.Brower, D.Kessler, J.Koplik and H.Levine, Phys. Rev. Lett., **51**, 1111 (1983); Phys. Rev.A, **29**, 1335 (1984)

[25] D.A.Kessler, J.Koplik and H.Levine, Phys. Rev.A, **30**, 3161 (1984)

[26] E.Ben-Jacob, N.D.Goldenfeld, B.G.Kotliar and J.S.Langer, Phys. Rev. Lett., **53**, 2110 (1984)

[27] D.Meiron, Phys. Rev.A, **33**, 2704 (1986)

[28] E.Ben-Jacob, P.Garik, T.Müller and D.Grier, Phys. Rev.A, **38**, 1370 (1988)

[29] See e.g. M.Wortis, In "Fundamental Problems in Statistical Mechanics", Proceedings of the 1984 Trondheim Summer School, Ed.: E.G.D.Cohen (North Holland, Amsterdam, 1985), p.87.

[30] M.Muschol, D.Liu and Z.Cummins, Phys.Rev.A, **46**, 1038 (1992)

[31] P.Oswald, F.Melo and C.Germain, J.Phys. France, **50**, 3527 (1989)

[32] H.Naito, M.Okuda and Ou-Yang Zhong-can, Phys.Rev.Lett., **70**, 2912 (1993)

[33] A.Buka, T.Tóth Katona and L.Kramer, Phys.Rev.E. **49**, 5271 (1994)

[34] J.S.Langer, in: Directions in Condensed Matter Physics, eds. G.Grinstein and G.Mazenko (World Science, 1986), pp. 164-186.

[35] A.A.Wheeler, B.T.Murray and R.J.Schaefer, Physica D, **66**, 243 (1993)

[36] A.Buka, T.Tóth Katona and L. Kramer, Accepted in Phys.Rev.E.

[37] A more detailed study of this substance will be published.

[38] A.Buka and N.Eber, Europhys. Lett., **21**(4), 477 (1993)

[39] P.Oswald, private communication

[40] P.Oswald, J.Malthete and P.Pelce, J. de Physique, **50**, 2121 (1989)

[41] A.Hernandez-Machado, R.Gonzalez-Cinca, L.Ramirez-Piscina and J.Casademunt, private communication